ELECTRON CLOUD MEASUREMENTS USING SHIELDED PICKUPS AT CESRTA*

J.P. Sikora†, J.A. Crittenden, J.S. Ginsberg, D.L. Rubin, CLASSE, Ithaca, New York, USA

Abstract

The Cornell Electron Storage Ring has been reconfigured as a test accelerator (CESRTA) with positron or electron beam energies ranging from 2 GeV to 5 GeV. An area of research at CESRTA is the study of the growth, decay and mitigation of electron clouds in the storage ring. Electron Cloud (EC) densities can be measured with a Shielded Pickup (SPU), where cloud electrons pass into the detector through an array of small holes in the wall of the beam-pipe. The signals produced by SPU have proved to be very useful in establishing the mitigating effect of different vacuum chamber surfaces - including differences in quantum efficiency as well as secondary and elastic yield. This has been accomplished through the careful comparison of observed signals with the output of the EC simulation code ECLOUD. We present example comparisons of data and simulation that show the sensitivity of the measurements to secondary and elastic yield. In addition, some data has been acquired using a solenoid to produce a longitudinal magnetic field at the SPU. We will also present our current understanding of the effect of a longitudinal magnetic field on SPU signals.

INTRODUCTION

An important feature of the Shielded Pickup (SPU) are the holes that connect its vacuum space to the that of the beam-pipe, as shown in Fig. 1. The holes have a depth to diameter ratio of about 3:1 that is effective in reducing the strength of the direct beam signal [1]. The holes also limit the angular acceptance of the detector, so that it is sensitive primarily to electrons with vertical trajectories.

Initial cloud electrons are generated when synchrotron radiation strikes the walls of the vacuum chamber producing photo-electrons. These electrons will then strike the wall and produce secondary electrons. There are three categories of secondary electrons [2]. The first is that of the true secondaries – where the incident electron interacts with the material in a non-trivial way and secondaries are produced. The two other categories are from scattering of an incident electron: elastics – where the energy of the secondary is equal to that of the incoming electron – and rediffused – electrons with energies up to the incident electron energy. Each of the categories has a corresponding secondary emission yield value, denoted by: δ_{ts}, δ_e and δ_r for true secondaries, elastic and rediffused respectively.
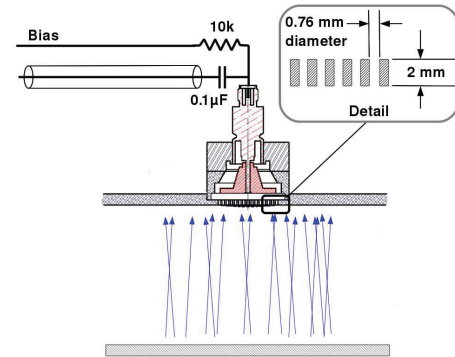
Figure 1: Cloud electrons enter the SPU through an array of small holes in the beam-pipe wall. The pickup is biased at +50 V and the signal amplified by +40 dB before being recorded by a digital oscilloscope.

Signals from the SPU are amplified and sent to an Agilent DSO6054 oscilloscope where they are digitized and averaged for 8k traces. The accelerator timing system provides triggers to the oscilloscope [3].

COMPARING DATA AND SIMULATION

Most of our experiments have focused on two bunch data, where bunches of equal population are injected into the storage ring with different spacings. As shown in Fig. 2, the signal from the second bunch is much larger than the first. The second bunch signal is dominated by electrons that were generated by the first bunch being kicked into the detector by the second bunch. So the signal after the second bunch represents a sample of the electron cloud that was produced by the first bunch.

The decay of the electron cloud is revealed by the superposition of a number of measurements with different bunch spacings. Through a comparison of these signals with simulations, the different spacings have shown different sensitivities to the three categories of secondary electrons.

Synchrotron radiation is simulated at the locations of the SPU with the program Synrad3D [4] that includes beam-pipe geometry and multiple diffuse scattering of photons throughout the CESR lattice. The simulation program ECLOUD [5, 6] uses the azimuthal photon absorption distribution to generate photo-electrons based on a parameterization of quantum efficiencies and photo-electron energies. The production of secondary electrons is based on the relative contributions from the three categories: true, rediffused and elastic. The vacuum chamber geometry and detector response is included in the model.
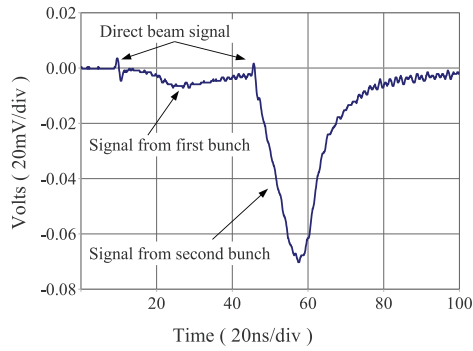
Figure 2: The SPU signal from two bunches of positrons, 36ns apart.

A comparison of measured signals and simulations with an uncoated aluminum chamber is shown in Figs. 3 and 4. The dotted lines are the measured signal and the points with (statistical) error bars are the simulation. The plots are a superposition of two bunch measurements similar to Fig. 2, but with six different bunch spacings.

The overall shape of the decay of the cloud is dominated by δ_0, the elastic yield δ_e as the energy of the incident electrons approaches zero (Fig. 3). Details of the signal from the first bunch are affected by changes in δ_r (Fig. 4).
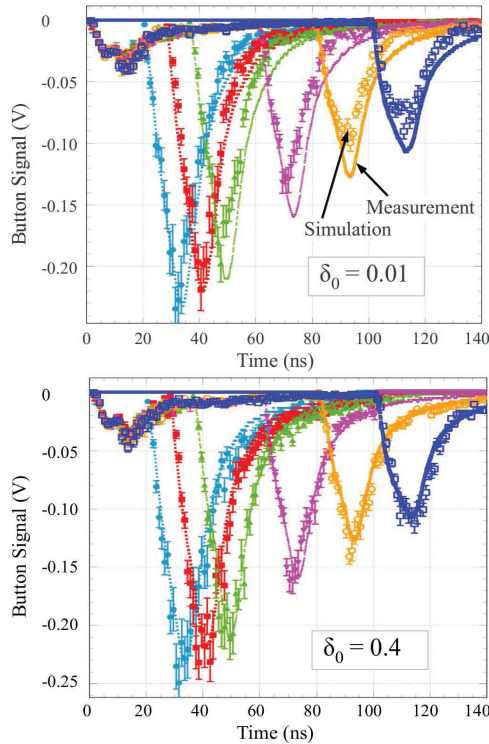

Figure 3: The effect of changing δ_0 in the simulation is shown above. The measured signal is shown as dots; the simulation as symbols with statistical error bars. The simulation fit is much better with a δ_0 of 0.4 (lower plot).
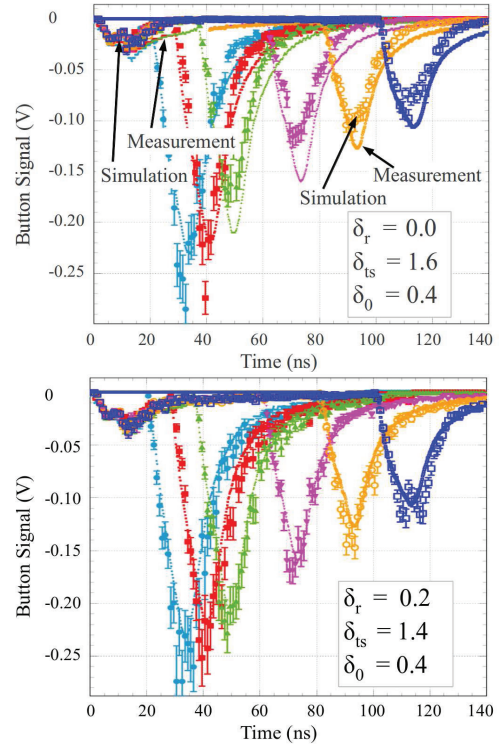

Figure 4: Changing the rediffused yield (δ_r) in the simulation increases the tail of the signal from the first bunch. In the upper plot, a near zero value of δ_r in the simulation does not match the data well. A larger value of δ_r gives a much better match and also affects the amplitude of the later second bunch signals.

SINGLE BUNCH WITH SOLENOID

Up to now, the flight time of cloud electrons has set the scale of photo-electron energy distributions in this analysis. The addition of a magnetic field should give additional information about the momentum of the electrons. Coils have been installed that can provide a longitudinal magnetic field in the region of the SPU detectors. Data with longitudinal magnetic field can be seen in Fig. 5. As the field increases up to 30 G, photo-electrons from the beam-pipe side wall begin to enter the detector as sketched in Fig. 7.

In Fig. 6, the peak voltage of the detector signal is plotted at each magnetic field setting over a range of $\pm$ 150 G. This was done at several different single bunch intensities from 1 to 10 mA (from 1.6×10^{10} to 1.6×10^{11} electrons/bunch). There is a significant asymmetry for positive and negative magnetic fields as might be expected with a synchrotron radiation stripe primarily on one side of the chamber. Analysis of this data is just beginning.

A simplified conceptual model of the SPU with a longitudinal field that contains the following ideas: the electrons entering the detector are those with nearly vertical trajectories so that they pass freely through the holes in the beam-pipe wall (see Fig. 1). As a result, with a longitudinal magnetic field the electrons entering the detector will follow trajectories that are circles with centers in the plane
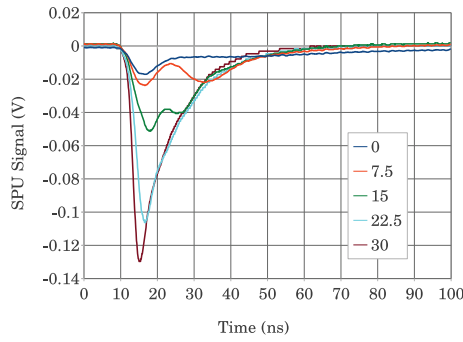
Figure 5: Data from the SPU with a 2 mA single bunch of electrons with a longitudinal field from 0 to 30 Gauss.

Figure 7: With longitudinal magnetic field, electrons entering the detector will follow circles in the plane of the holes.
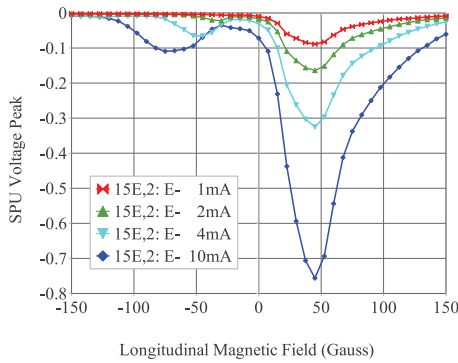

Figure 6: The peak value of the SPU signal is plotted at each magnetic field setting. This was done with single electron bunch intensities from 1 to 10 mA.

Figure 8: A simulation of the electron cloud signal from a single bunch in a longitudinal magnetic field of 23 Gauss with rectangular beam-pipe shows peaks that correspond to multiples of a quarter cyclotron period.

of the detector holes as shown in Fig. 7.

Another important constraint is that the amount of time for non-relativistic electrons to complete a cycle (or fixed portion of a cycle) is determined by their cyclotron period $\tau_{cyc} = 2\pi m_e/qB$. This time is independent of the energy of the electrons. The beam-pipe was also simplified in this model to be rectangular. As can be seen in Fig. 7, any electrons that come from the top surface of the rectangular beam-pipe will arrive in a half cyclotron period, those from the bottom will arrive in less than a quarter period, and those from the side wall something between a half and a quarter period. So at a given magnetic field, the arrival time of photo-electrons is determined mostly by their point of origin rather than their energy.

An ECLOUD simulation of rectangular beam-pipe was run with a realistic synchrotron light distribution that included scattered photons. Its output agreed with the conceptual model by showing three signal peaks that corresponded to photo-electrons from the midpoint of the side wall, another from the top of the beam-pipe and a broad peak from secondary electrons produced on the ceiling as shown in Fig. 8.

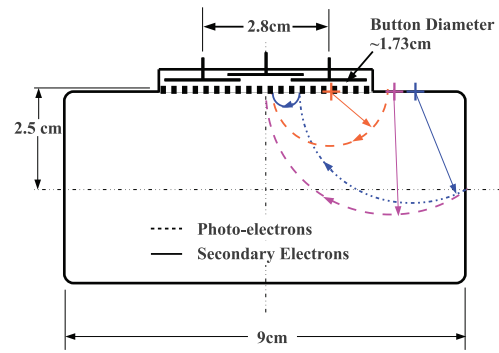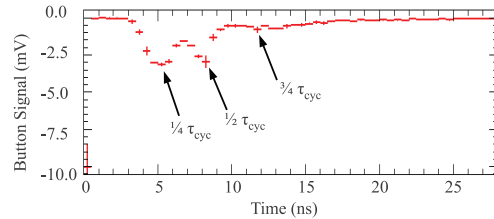Simulations that also included existing beam-pipe geometry (non-rectangular) did not agree with the data until adjustments were made to the photo-electron energy distributions. Work is continuing in order to establish the simulation parameters that will yield good agreement with data over a wide range of magnetic field values and beam energies.

REFERENCES

[1] M. Sands, "Energy Loss from Small Holes in the Vacuum Chamber,", PEP-253, Sept. 1977.

[2] M. A. Furman & M. T. F. Pivi, "Probabilistic Model for the Simulation of Secondary Electron Emission," *Phys. Rev. ST Accel. Beams* **5**, 124404 (Dec. 2002).

[3] J. P. Sikora, *et al.*, "Time Resolved Measurement of Electron Clouds at CESRTA Using Shielded Pickups ," in Proc. of PAC'11, New York, NY, USA, August 2011, WEP195, p.1855, (2011).

[4] G. Dugan & D. Sagan, "Synrad3D Photon Propagation and Scattering Simulation," *49th ICFA Advanced Beam Dynamics Workshop on Electron Cloud Physics*, Ithaca, NY, K. Smolenski, Ed. (in press), Paper PST08.

[5] F. Zimmermann, G. Rumolo and K. Ohmi, in *ICFA Beam Dynamics Newsletter*, K. Ohmi & M. Furman, Eds., International Committee on Future Accelerators, No. 33, p. 14-24 (Apr. 2004).

[6] J.A. Crittenden, *et al.*, "Electron Cloud Modeling Results for Time-resolved Shielded Pickup Measurements at CESRTA," in Proc. of PAC'11, New York, NY, USA, August 2011, WEP142, p.1752, (2011).